

CaV3.1 T-Type Ca²⁺ Channels Contribute to Myogenic Signalling in Rat Retinal Arterioles

Fernandez, J. A., McGahon, M. K., McGeown, J. G., & Curtis, T. M. (2015). CaV3.1 T-Type Ca²⁺ Channels Contribute to Myogenic Signalling in Rat Retinal Arterioles. *Investigative Ophthalmology and Visual Science*, 56(9), 5125-5132. DOI: 10.1167/iovs.15-17299

Published in:
Investigative Ophthalmology and Visual Science

Document Version:
Peer reviewed version

Queen's University Belfast - Research Portal:
[Link to publication record in Queen's University Belfast Research Portal](#)

Publisher rights
Copyright 2015 The Association for Research in Vision and Ophthalmology, Inc.

General rights
Copyright for the publications made accessible via the Queen's University Belfast Research Portal is retained by the author(s) and / or other copyright owners and it is a condition of accessing these publications that users recognise and abide by the legal requirements associated with these rights.

Take down policy
The Research Portal is Queen's institutional repository that provides access to Queen's research output. Every effort has been made to ensure that content in the Research Portal does not infringe any person's rights, or applicable UK laws. If you discover content in the Research Portal that you believe breaches copyright or violates any law, please contact openaccess@qub.ac.uk.

1 **Ca_v3.1 T-Type Ca²⁺ Channels Contribute to Myogenic Signalling in**
2 **Rat Retinal Arterioles**

3

4 José A. Fernández*, Mary K. McGahon, J. Graham McGeown and Tim M. Curtis *¹

5 Centre for Experimental Medicine, Queen's University of Belfast

6 *These authors contributed equally as senior authors.

7 ¹Corresponding author:

8 Dr Tim Curtis
9 Centre for Experimental Medicine
10 Queen's University of Belfast
11 Institute of Clinical Sciences Block A
12 Grosvenor Road
13 Royal Victoria Hospital
14 Belfast
15 BT12 6BA
16 Tel: +44 (0) 2890635027
17 Email: t.curtis@qub.ac.uk

18

19 Word count: 3693

20 Supported by grants from British Heart Foundation (PG/11/94/29169) and
21 Biotechnology and Biological Sciences Research Council (BB/I026359/1).

22 **Abstract**

23 **Purpose:** Although L-type Ca^{2+} channels are known to play a key role in the
24 myogenic reactivity of retinal arterial vessels, the involvement of other types of
25 voltage-gated Ca^{2+} channels in this process remains unknown. In the present study
26 we have investigated the contribution of T-type Ca^{2+} channels to myogenic signalling
27 in arterioles of the rat retinal microcirculation.

28 **Methods:** Confocal immunolabelling of wholemount preparations was used to
29 investigate the localisation of $\text{Ca}_v3.1-3$ channels in retinal arteriolar smooth muscle
30 cells. T-type currents and the contribution of T-type channels to myogenic signalling
31 were assessed by whole-cell patch-clamp recording and pressure myography of
32 isolated retinal arteriole segments.

33 **Results:** Strong immunolabelling for $\text{Ca}_v3.1$ was observed on the plasma membrane
34 of retinal arteriolar smooth muscle cells. In contrast, no expression of $\text{Ca}_v3.2$ or
35 $\text{Ca}_v3.3$ could be detected in retinal arterioles, although these channels were present
36 on glial cell end-feet surrounding the vessels and retinal ganglion cells, respectively.
37 TTA-A2-sensitive T-type currents were recorded in retinal arteriolar myocytes with
38 biophysical properties distinct from those of the L-type currents present in these
39 cells. Inhibition of T-type channels using TTA-A2 or ML-218 dilated isolated,
40 myogenically active, retinal arterioles.

41 **Conclusions:** $\text{Ca}_v3.1$ T-type Ca^{2+} channels are functionally expressed on arteriolar
42 smooth muscle cells of retinal arterioles and play an important role in myogenic
43 signalling in these vessels. The work has important implications concerning our
44 understanding of the mechanisms controlling blood flow autoregulation in the retina
45 and its disruption during ocular disease.

46 **Introduction**

47 It has long been known that alterations in perfusion pressure generate compensatory
48 changes in the diameters of retinal vessels that result in minor or no effects on
49 overall retinal blood flow.¹ A reduced ability of the retina to autoregulate in this
50 manner has been associated with a number of ocular diseases including diabetes,
51 glaucoma and age-related macular degeneration (AMD).²⁻⁶ Vascular autoregulation
52 in the retina is driven by a number of different mechanisms, with both myogenic and
53 metabolic components involved.⁷ The importance of myogenic mechanisms in the
54 regulation of retinal blood flow has been highlighted by several studies performed on
55 isolated retinal arteries and arterioles, showing vasoconstriction or vasodilation in
56 response to either increases or decreases in intravascular pressure, respectively.⁸⁻¹¹

57 According to the classical view, myogenic responses occur when
58 pressure-induced distension of the vessel wall triggers activation of stretch-activated
59 cation channels on the resident vascular smooth muscle cells, resulting in cell
60 membrane potential depolarisation and increased Ca^{2+} influx through
61 voltage-operated L-type Ca^{2+} channels.¹²⁻¹⁴ This Ca^{2+} influx in turn leads to vascular
62 smooth muscle cell contraction and vessel constriction both directly by increasing the
63 cytosolic Ca^{2+} concentration and indirectly by triggering the release of Ca^{2+} from the
64 sarcoplasmic reticulum via ryanodine (RyR) and inositol trisphosphate receptor
65 channels.¹²⁻¹⁴ We have previously shown that L-type Ca^{2+} channels and RyR
66 receptors play a key role in myogenic signalling in retinal arterioles.^{10,11} These
67 vessels also express voltage-gated $\text{K}_v1.5$ channels^{11,15} and large-conductance Ca^{2+} -
68 activated K^+ channels (BK channels)^{11,16} which act as a brake on the myogenic
69 response mechanism by limiting the degree of pressure-induced depolarisation.
70 Ca^{2+} -activated Cl^- channels have also been found to contribute to the contractile

71 state of these vessels, although their primary role appears to be in the modulation of
72 agonist-induced tone, rather than myogenic signalling.^{17,18}

73 Recent studies in other vascular beds have suggested that additional ion
74 channels, such as T-type Ca^{2+} channels, might function as alternative
75 voltage-dependent Ca^{2+} influx pathways that may be involved in the development
76 and maintenance of myogenic tone.^{19,20} Molecular analyses have identified three
77 different isoforms of pore-forming T-type Ca^{2+} channels, namely $\text{Ca}_v3.1$, $\text{Ca}_v3.2$ and
78 $\text{Ca}_v3.3$.^{21,22} Several studies have found some of these to be expressed and
79 functional in resistance vessels,^{23–25} contributing in some cases to myogenic
80 signalling.^{20,23,26–28} T-type Ca^{2+} channels appear to be particularly important in
81 mediating myogenic responses in small arterioles where, despite a loss or decrease
82 in L-type Ca^{2+} currents, development of myogenic tone is still observed.^{26,29,30}

83 In the present study, we have investigated for the first time the possible
84 involvement of T-type Ca^{2+} channels in the myogenic reactivity of rat retinal
85 arterioles. Using immunohistochemistry, we show that although all three T-type Ca^{2+}
86 channel isoforms are expressed in retinal tissue, only $\text{Ca}_v3.1$ localises to retinal
87 arteriolar smooth muscle cells. We also demonstrate the functional expression of T-
88 type Ca^{2+} channels on the plasma membrane of these cells and characterise their
89 biophysical and pharmacological properties. Finally, we show that two structurally
90 distinct T-type Ca^{2+} channel blockers dilate isolated pressurised retinal arterioles
91 under conditions of steady state myogenic tone, suggesting that these channels
92 make a significant contribution to myogenic signalling in these vessels. These
93 findings have important implications for our understanding of the mechanisms
94 controlling retinal blood flow in both health and disease.

95 **Methods**

96 Animal use conformed to the standards in the ARVO Statement for the Use of
97 Animals in Ophthalmic and Vision Research. Male Sprague-Dawley rats (8–12
98 weeks of age; 200–250g; Harlan, Bicester, UK) were euthanized with CO₂ in
99 accordance with guidelines contained within the UK Animals (Scientific Procedures)
100 Act of 1986 and approved by the Queen’s University of Belfast Animal Welfare and
101 Ethical Review Body.

102

103 ***Immunohistochemistry***

104 Immunohistochemistry was carried out on retinal arterioles embedded within retinal
105 flatmount preparations as described previously.¹⁶ Briefly, freshly enucleated eyes
106 were placed in low Ca²⁺ Hanks solution (see Drugs and Solutions) and hemisected
107 along the ora serrata. The vitreous was removed and the posterior eyecup fixed with
108 4% paraformaldehyde (PFA) for 20 minutes and then washed extensively in
109 phosphate buffered saline (PBS) for 1 hour. Retinas were subsequently detached
110 and incubated overnight in permeabilisation and blocking buffer (0.05% Triton X-100
111 and 1% donkey serum in PBS; Sigma, Poole, Dorset, UK, and Millipore, Watford,
112 UK) and then incubated in primary antibody in permeabilisation and blocking buffer
113 for 3 days at 4°C. Primary antibodies, selected on the basis of their specificity
114 towards rat Ca_v3.1–3 channels (Table 1) were employed in conjunction with mouse
115 anti- α -smooth muscle actin (α SMA) antibody (1:200; Sigma) to positively identify
116 vascular smooth muscle cells or isolectin B4 (1:50; Sigma)³¹ to label vascular plasma
117 membranes. Following extensive washing (4 hours at 21°C in PBS), donkey anti-
118 rabbit IgG labelled with Alexa-488 (Life Technologies, Paisley UK; 1:200 in
119 permeabilisation and blocking buffer) or Streptavidin 568 (Life Technologies; 1:500)

120 were used for Ca_v3.1–3 channel and vascular cell membrane detection, respectively
121 (incubated 4°C overnight). The αSMA primary antibody was conjugated to Cy3, so
122 no secondary antibody was required. Nuclei were labelled with the far-red nuclear
123 stain TOPRO3 (1:1000; Life Technologies; pseudo-coloured blue in relevant
124 images). The immunohistochemistry for each of the Ca_v3.1–3 isoforms was repeated
125 using 4–8 retinas from at least 4 different animals. Secondary only controls and
126 blocking peptide experiments for Ca_v3.1 (10μg/ml blocking peptide) were also
127 performed. Images were acquired using a Leica SP5 confocal laser scanning
128 microscope (Leica Geosystems; Heerbrugg, Switzerland; HCX PL APO 63x OIL
129 immersion lens) equipped with Argon, HeNe 543 and HeNe 633 lasers. Images were
130 captured in sequential scanning mode with emission wavelengths appropriate for the
131 fluorophores used to reduce overlap (bleed-through) of signals.

132

133 ***Isolated Arteriolar Preparation***

134 For electrophysiology and pressure myography experiments, isolated retinal arteriole
135 segments were used.³² Retinas were dissected from freshly enucleated eyes, placed
136 in low Ca²⁺ Hanks' solution and mechanically triturated using a fire-polished Pasteur
137 pipette. Homogenate was pipetted into a glass-bottomed recording bath mounted on
138 an inverted microscope (Eclipse TE300; Nikon, Tokyo, Japan) and isolated retinal
139 arterioles (length, 100–4000 μm; outer diameter, 15–40 μm) anchored down with
140 tungsten wire slips as described previously.¹⁶ Arterioles were continuously
141 superfused with normal Hanks' solution at 37°C during experimentation. Drugs were
142 delivered via a gravity-fed multi-channel perfusion manifold connected to a single
143 outlet needle that was positioned adjacent to the vessel of interest.

144

145 ***Electrophysiological Recordings***

146 Whole-cell membrane currents were recorded from individual arteriolar smooth
147 muscle cells still embedded within their parental arterioles using the perforated
148 patch-clamp technique.³³ Prior to patching, the vessels were superfused with
149 collagenase 1A (0.1 mg/ml, 10 minutes; Sigma), protease type XIV (0.01 mg/ml, 10
150 minutes; Sigma) and DNase I (0.02 mg/ml, 5 minutes; Millipore) in low Ca²⁺ Hanks'
151 solution to remove surface basal lamina, electrically uncouple endothelial cells from
152 overlying arteriolar smooth muscle cells and individual smooth muscle cells from one
153 another, and to remove extraneous DNA.^{15,33} Once the whole-cell perforated
154 configuration was acquired, the external Hanks' solution was switched to divalent
155 free solution (see Drugs and Solutions) to enhance the magnitude of currents flowing
156 through voltage-gated Ca²⁺ channels and to prevent interference by Ca²⁺-activated
157 Cl⁻ currents.^{34,35} Pipettes pulled from filamented borosilicate glass capillaries (1.5
158 mm o.d. w 1.17 mm i.d., Harvard Instruments, Kent, UK) were fire polished to
159 resistances of 1-2 MΩ. Membrane currents were recorded using an Axopatch 200B
160 patch-clamp amplifier (Molecular Devices, CA, USA), low pass filtered at 0.5 kHz
161 and sampled at 2 kHz. Voltage step protocols were applied using pClamp (version
162 10.2; Molecular Devices) via a Digidata 1440A interface (Molecular Devices). Leak
163 currents were subtracted off-line from the active currents using the response to a
164 hyperpolarizing step from a holding potential of -80 mV to -90 mV as the correction
165 signal. Calculation and plotting of difference curves, off-line leak subtraction and
166 fitting of exponentials was performed using purpose-written software in R.³⁶

167 ***Arteriolar Myography***

168 The involvement of T-type Ca²⁺ channels in the generation of arteriolar myogenic
169 tone was assessed using pressure myography as previously described.¹⁶ A tungsten

170 wire slip was laid on the arteriole, anchoring and occluding one end. The vessel was
171 then superfused with Ca^{2+} -free Hanks' solution. The open end was cannulated using
172 a glass micropipette (1.5mm o.d., 0.86 i.d. tapered to a tip diameter of 2–5 μm) filled
173 with Ca^{2+} -free Hanks' solution, using a patch-clamp electrode holder and
174 micromanipulator (Molecular Devices). Once the pipette tip had been appropriately
175 positioned, the pipette was advanced so as to wedge it tightly into the lumen of the
176 vessel. To ensure there was no significant flow through the vessel or leakage of fluid
177 around the cannulation site, a small air bubble was introduced into the tubing
178 connecting the cannulating pipette to the manometer. Only vessels where this
179 bubble remained relatively static following pressurisation were used for
180 experimentation. Following introduction of the pipette, the vessel was superfused
181 with normal Hanks' solution for 10–15 minutes, allowing the pipette to seal to the
182 inner vessel wall. Vessels were then pressurised to 40 mmHg and left at that
183 pressure until stable myogenic tone had fully developed (usually ~10 minutes).
184 Intraluminal pressure was regulated by using a manometer connected to the
185 cannulating micropipette (Riester "Big Ben" pressure manometer; Riester,
186 Jungingen, Germany). The maximum passive diameter of the vessels was
187 determined by application of the myosin light chain kinase inhibitor, wortmannin (10
188 μM),^{37,38} in the presence of Ca^{2+} -free Hanks' solution at the end of the experiment.
189 This value was used to normalise vessel diameter data across individual arterioles.
190 Vessels were viewed under a 20x, NA 0.4 objective and images (saved as BMP
191 images of 1280x1024 pixels; 8-bit; 1.2MB) captured at a rate of 140 images per
192 minute using a MCN-B013-U USB camera (Mightex, Pleasanton, CA, USA).
193 Acquisition was carried out using custom software implemented in Delphi.¹⁶ The

194 measurement of vessel diameters and tracking of diameter changes was performed
195 using the MyoTracker software package.³⁹

196

197 ***Drugs and Solutions***

198 The composition of the solutions used was as follows (in mM): Normal Hanks'
199 solution - 140, NaCl; 6, KCl; 5, D-glucose; 2, CaCl₂; 1.3, MgCl₂; 10, HEPES; pH set
200 to 7.4 with NaOH; Divalent free solution - 120, NaCl; 5, KCl; 5, D-glucose; 10,
201 HEPES; 5, EGTA; 20, Tetraethylammonium Chloride (TEA); K⁺-based internal
202 pipette solution; 52, KCl; 80, Gluconic acid; 80, KOH; 1, MgCl₂; 0.5, EGTA; 10,
203 HEPES; pH set to 7.2 with KOH. The low Ca²⁺ Hanks' solution was of Hanks'
204 composition, but contained only 0.1 mM Ca²⁺. For the Ca²⁺ free Hanks' solution,
205 Ca²⁺ was omitted. Amphotericin B (final concentration of 0.39 mM) was dissolved in
206 the pipette solutions as the pore-forming agent.

207 Unless otherwise stated, stock solutions of drugs were initially prepared in
208 DMSO and then diluted to the final concentration. The final bath concentration of
209 DMSO was ≤0.1%. In vehicle control experiments, application of DMSO, at the
210 maximal concentration used in these studies, had no effect on arteriolar diameter
211 (Table 2). Amphotericin B, nimodipine, TEA and EGTA were obtained from Sigma;
212 TTA-A2, ML-218 and wortmannin were purchased from Alomone Labs (Jerusalem,
213 Israel). HEPES was obtained from Melford Laboratories (Ipswich, UK).

214

215 ***Statistical Analysis***

216 Data are presented as the mean ± SEM. Statistical significance was determined by
217 using either paired t-tests (when data conformed to Kolmogorov-Smirnov normality

218 tests) or the Wilcoxon matched-pairs signed rank test for which no assumptions
219 about normality were made. In all comparisons, the 95% level was accepted as
220 statistically significant. Analysis was carried out using Prism 5 for Windows (version
221 5.03; GraphPad Software Inc., La Jolla, CA, USA). In all graphical representations of
222 the data, statistical significance is indicated as follows: NS, $P > 0.05$; $* = P < 0.05$;
223 $** = P < 0.01$; $*** = P < 0.001$.

224

225 **Results**

226 ***Immunolocalisation of T-Type Ca²⁺ Channels in Retinal Arteriolar Smooth***
227 ***Muscle***

228 The expression of the three T-type channel isoforms, Ca_v3.1, Ca_v3.2 and Ca_v3.3,
229 was examined in rat retinal wholemount preparations using immunohistochemistry.
230 Retinal arterioles were identified by positive staining for αSMA with a single
231 monolayer of vascular smooth muscle cells running transversely to the long axis of
232 the vessels (Fig. 1 A). In contrast, venules showed much weaker αSMA staining of
233 pericyte-like mural cells (Fig. 1 B). As shown in Figure 2, strong immunolabelling for
234 Ca_v3.1 proteins was detected on the surface of the retinal arteriolar smooth muscle
235 cells, along with weaker, more diffuse, cytosolic staining (Fig. 2 A). Plasma
236 membrane expression of Ca_v3.1 channels was confirmed by co-localisation with
237 isolectin B4 (Fig. 2 B). In the surrounding retinal neuropile, Ca_v3.1 expression was
238 also localised to retinal ganglion cells (RGCs; Fig. 2 A). Control experiments
239 performed with secondary antibodies only or primary anti-Ca_v3.1 antibodies
240 pre-absorbed with a specific blocking peptide were negative (Fig. 2 C). Expression of
241 Ca_v3.2 was detected in close proximity to the retinal arterioles (Fig. 2 D). However,
242 on closer inspection, it was evident that this expression was limited to the
243 perivascular end-feet of glial cells surrounding the vessels. Ca_v3.3 expression was
244 absent from retinal arterioles, but strong immunolabelling was present in the
245 surrounding retinal neuropile primarily associated with RGCs (Fig. 2 E).

246

247

248 **Electrical Characterisation of the T-Type Currents**

249 Whole-cell patch-clamp experiments were conducted to examine the functional
250 expression of T-type Ca^{2+} channels on the plasma membrane of retinal arteriolar
251 smooth muscle cells. Figure 3 shows voltage-dependent inward T-type currents
252 sensitive to external application of the selective T-type Ca^{2+} channel inhibitor, TTA-
253 A2 (1 μM ; Fig. 3 A, left panel),^{40,41} and L-type currents sensitive to nimodipine (1 μM ;
254 Fig. 3 A, right panel)¹⁰. Representative and average current-voltage (*I-V*)
255 relationships for both TTA-A2- and nimodipine-sensitive currents are also shown
256 (Fig. 3 B, left and right panels, respectively). As can be seen, the TTA-A2-sensitive
257 *I-V* curve activates at a more negative membrane potential than the
258 nimodipine-sensitive current (-70 mV for the T-type current compared to -50 mV for
259 the L-type current; Fig. 3 B). This is also the case for the peak currents, with T-type
260 current peaking at around -30 to -20 mV, compared to -10 to 0 mV for the L-type
261 current (Fig. 3 B). These currents also displayed significant differences in their rates
262 of activation and inactivation, with the T-type currents having a faster rate of both
263 activation (T_{ac} 4.3 ± 0.7 versus 8.2 ± 1.3 ms) and inactivation (T_{inac} 18.2 ± 1 versus
264 24.1 ± 1.5 ms) compared with the L-type currents ($P < 0.01$ in both cases, $n = 8$; Fig. 3
265 C and D). Thus, these results confirm that T-type Ca^{2+} channels are functionally
266 expressed in retinal arteriolar smooth muscle cells, and in the final experiments,
267 analyses were performed to examine their possible role in the myogenic reactivity of
268 retinal arterioles.

269

270

271 ***Blocking T-Type Ca²⁺ Channels Causes Dilation of Pressurised Retinal***
272 ***Arterioles***

273 To investigate the possible role of T-type channels in myogenic signalling, we carried
274 out pressure myography experiments on isolated retinal arterioles. Vessels were
275 cannulated and pressurised to 40 mmHg until myogenic tone had fully developed
276 and stabilised. Arterioles were then exposed to TTA-A2 (1 µM) or another selective
277 T-type Ca²⁺ channel blocker, ML-218 (1 µM),⁴² and changes in vessel diameter
278 recorded. At the end of the experiment, wortmannin (10 µM), was applied in Ca²⁺-
279 free Hanks' solution in order to obtain the maximal passive diameter of the vessels.
280 Both TTA-A2 and ML-218 caused a significant dilation of myogenically active rat
281 retinal arterioles by ~50% of the maximal passive diameter (P<0.001, Wilcoxon
282 matched-pairs signed rank test; Fig. 4 A and B, Table 2). These findings are
283 consistent with the view that T-type Ca²⁺ channels contribute to the generation of
284 myogenic tone in these vessels.

285

286

287 **Discussion**

288 This study shows for the first time that the T-type Ca^{2+} channel isoform, $\text{Ca}_v3.1$, is
289 functionally expressed in vascular smooth muscle cells of rat retinal arterioles and
290 plays an important role in myogenic signalling in these vessels. Although we found
291 no evidence for expression of $\text{Ca}_v3.2$ or $\text{Ca}_v3.3$ channels in these vessels, these
292 isoforms were identified in glial cell end-feet surrounding the vessels ($\text{Ca}_v3.2$; Fig. 2
293 D) and RGCs ($\text{Ca}_v3.3$; Fig. 2 E). Our results are consistent with previous studies
294 reporting $\text{Ca}_v3.1$ expression in vascular smooth muscle cells of other vascular beds,
295 including those of the renal, skeletal muscle, mesenteric, brain and pulmonary
296 circulations.^{23,24,27,30,43–45} Although expression of $\text{Ca}_v3.3$ has not been widely
297 reported in vascular smooth muscle cells, $\text{Ca}_v3.2$ has been detected in cerebral and
298 pulmonary artery myocytes.^{20,45} Recent work has established that Ca^{2+} influx through
299 vascular smooth muscle $\text{Ca}_v3.2$ channels is principally involved in mediating
300 vasodilatory responses via activation of RyR-dependent Ca^{2+} sparks and BK
301 channels.²⁸ It would appear unlikely, however, that such a mechanism is active in
302 retinal arterioles, given that $\text{Ca}_v3.2$ channels could not be detected in these vessels.

303 Consistent with the presence of $\text{Ca}_v3.1$ channels on the plasma membrane of
304 retinal arteriolar myocytes, we identified T-type currents with pharmacological and
305 kinetic features similar to those produced by $\text{Ca}_v3.1$ subunits in other systems (Fig.
306 3).^{21,46} These currents were different from the L-type voltage-dependent Ca^{2+}
307 currents in these cells in that they were activated at lower membrane potentials and
308 had faster kinetic rates of activation and inactivation (Fig. 3). Similar kinetic rates
309 have been reported for T-type channels in other vascular tissues.^{21,28,47} Some
310 studies carried out on mesenteric and cerebral arteries, however, have reported an
311 unexpected depolarising shift in the activation and inactivation profiles of these

312 channels compared to traditional T-type channels, leading to the suggestion that in
313 vascular myocytes the T-type channels may be formed from splice variants.⁴⁸ In our
314 study, however, we could detect two clearly distinguishable peaks in the *I-V* curves
315 for T-type and L-type currents, closer to traditional T-type values, and the peak *I-V*
316 values shown here (–30 to –20 mV) closely match those reported for T-type currents
317 in other cells, including neurons, cardiomyocytes and coronary and aortic vascular
318 smooth muscle cells.²¹

319 Although L-type Ca²⁺ channels are generally believed to play a central role in
320 the development of myogenic tone,¹³ it has been noted in several studies that L-type
321 Ca²⁺ channel inhibition does not completely abolish the myogenic response.^{19,20,49–51}
322 In the present study, we have demonstrated that two different T-type blockers,
323 TTA-A2 and ML-218, are capable of partially inhibiting myogenic signalling in
324 isolated rat retinal arterioles (Fig. 4; Table 2). Whilst the absolute changes in vessel
325 diameter that we have recorded following T-type Ca²⁺ channel blockade are
326 relatively small, we have calculated for individual arterioles that these would be
327 expected to decrease vascular resistance in the range of ~3-15% (mean of ~7%;
328 based on $R \propto 1/d^4$).¹⁰ Thus it seems likely that these channels will make at least some
329 contribution to the modulation of retinal blood flow autoregulation *in vivo*. Our data
330 concur with other studies showing that Ca_v3.1 T-type channels play an important
331 role in the development and maintenance of myogenic tone in vessels from several
332 vascular beds. Navarro-Gonzalez et al. (2009), for example, showed that myogenic
333 tone in the rat basilar artery results from Ca²⁺ influx through nifedipine-insensitive
334 voltage-dependent Ca²⁺ channels with characteristics similar to the T-type channel
335 isoform Ca_v3.1.⁴³ Björling et al. (2013), working with mice deficient in the Ca_v3.1 T-
336 type isoform, showed that T-type channels are crucial for myogenic tone in

337 mesenteric arteries at low arterial pressure (<80 mmHg), but are inactivated at high
338 arterial pressure where L-type Ca^{2+} channels predominate in the myogenic
339 response.^{20,52-54} Since the arterial input pressure in the retina is thought to be ~40
340 mmHg,^{55,56} and retinal arterioles exhibit myogenic tone between 10 and 70
341 mmHg,^{9,10,57} these observations would support the view that $\text{Ca}_v3.1$ T-type channels
342 are likely to play an important role in both setting basal vascular tone and in
343 modulating vascular tone in response to changes in systemic blood pressure (i.e. in
344 mediating blood flow autoregulation) in the retinal microcirculation *in vivo*.

345 In summary, this study is the first to identify $\text{Ca}_v3.1$ T-type currents in vascular
346 smooth muscle cells of retinal arterioles and to characterise their contribution to
347 myogenic signalling in these vessels. The work provides an important foundation for
348 better understanding the mechanisms regulating retinal perfusion in both health and
349 disease. It seems likely, for example, that in addition to contributing to the myogenic
350 reactivity of retinal arterioles, endothelial and glial cell mediators known to modulate
351 retinal vascular tone and blood flow may, at least in part, act by targeting the activity
352 of these channels. In support of this idea, previous studies have shown that
353 vasodilator molecules such as nitric oxide and 5,6 epoxyeicosatrienoic acid are
354 capable of inhibiting T-type Ca^{2+} channel activity,^{58,59} while the vasoconstrictor
355 peptide, endothelin-1, has been shown to enhance currents through these
356 channels.⁶⁰ From a pathophysiological perspective, we currently have only a limited
357 knowledge of the role of T-type Ca^{2+} currents in the development of vascular
358 disease, although $\text{Ca}_v3.1$ channels have been identified as potential therapeutic
359 targets for the prevention of restenosis following angioplasty.⁶¹ Our current work
360 opens up several new avenues for further research. The possibility that alterations in
361 $\text{Ca}_v3.1$ channel expression and activity contribute to the loss of retinal vascular

362 autoregulation and blood flow disturbances during diseases such as diabetes,
363 glaucoma and AMD now merits further investigation.

364

365 **References**

- 366 1. Robinson F, Riva CE, Grunwald JE, Petrig BL, Sinclair SH. Retinal blood flow
367 autoregulation in response to an acute increase in blood pressure. *Invest*
368 *Ophthalmol Vis Sci.* 1986;27:722–726.
- 369 2. Anderson DR. Introductory comments on blood flow autoregulation in the optic
370 nerve head and vascular risk factors in glaucoma. *Surv Ophthalmol.* 1999;43:S5–S9.
- 371 3. Evans DW, Harris A, Garrett M, Chung HS, Kagemann L. Glaucoma patients
372 demonstrate faulty autoregulation of ocular blood flow during posture change. *Br J*
373 *Ophthalmol.* 1999;83:809–813.
- 374 4. Ehrlich R, Harris A, Kheradiya NS, Winston DM, Ciulla TA, Wirostko B. Age-
375 related macular degeneration and the aging eye. *Clin Interv Aging.* 2008;3:473–
376 482.
- 377 5. Pemp B, Schmetterer L. Ocular blood flow in diabetes and age-related macular
378 degeneration. *Can J Ophthalmol.* 2008;43:295–301.
- 379 6. He Z, Vingrys AJ, Armitage JA, Bui BV. The role of blood pressure in glaucoma.
380 *Clin Exp Optom.* 2011;94:133–149.
- 381 7. Pournaras CJ, Rungger-Brandle E, Riva CE, Hardarson SH, Stefansson E.
382 Regulation of retinal blood flow in health and disease. *Prog Retin Eye Res.*
383 2008;27:284–330.
- 384 8. Hoste AM, Boels PJ, Brutsaert DL, De Laey JJ. Effect of alpha-1 and beta
385 agonists on contraction of bovine retinal resistance arteries in vitro. *Invest*
386 *Ophthalmol Vis Sci.* 1989;30:44–50.
- 387 9. Delaey C, Van de Voorde J. Pressure-induced myogenic responses in isolated
388 bovine retinal arteries. *Invest Ophthalmol Vis Sci.* 2000;41:1871–1875.
- 389 10. Kur J, Bankhead P, Scholfield CN, Curtis TM, McGeown JG. Ca(2+) sparks
390 promote myogenic tone in retinal arterioles. *Br J Pharmacol.* 2013;168:1675–1686.
- 391 11. Kur J, McGahon MK, Fernández JA, Scholfield CN, McGeown JG, Curtis TM.
392 Role of ion channels and subcellular Ca²⁺ signaling in arachidonic acid-induced
393 dilation of pressurized retinal arterioles. *Invest Ophthalmol Vis Sci.* 2014;55:2893–
394 2902.
- 395 12. Gollasch M, Nelson MT. Voltage-dependent Ca²⁺ channels in arterial smooth
396 muscle cells. *Kidney Blood Press Res.* 1997;20:355–371.
- 397 13. Davis MJ, Hill MA. Signaling mechanisms underlying the vascular myogenic
398 response. *Physiol Rev.* 1999;79:387–423.

- 399 14. Catterall WA. Voltage-gated calcium channels. *Cold Spring Harb Perspect Biol.*
400 2011;3:a003947.
- 401 15. McGahon MK, Dawicki JM, Arora A, et al. Kv1.5 is a major component
402 underlying the A-type potassium current in retinal arteriolar smooth muscle. *Am J*
403 *Physiol Heart Circ Physiol.* 2007;292:H1001–H1008.
- 404 16. McGahon MK, Dash DP, Arora A, et al. Diabetes downregulates large-
405 conductance Ca²⁺-activated potassium β 1 channel subunit in retinal arteriolar
406 smooth muscle. *Circ Res.* 2007;100:703–711.
- 407 17. McGahon MK, Needham MA, Scholfield CN, McGeown JG, Curtis TM. Ca²⁺-
408 activated Cl⁻ current in retinal arteriolar smooth muscle. *Invest Ophthalmol Vis Sci.*
409 2009;50:364–371.
- 410 18. Needham M, McGahon MK, Bankhead P, et al. The role of K⁺ and Cl⁻ channels
411 in the regulation of retinal arteriolar tone and blood flow. *Invest Ophthalmol Vis Sci.*
412 2014;55:2157–2165.
- 413 19. Mufti RE, Brett SE, Tran CH, et al. Intravascular pressure augments cerebral
414 arterial constriction by inducing voltage-insensitive Ca²⁺ waves. *J Physiol.*
415 2010;588:3983–4005.
- 416 20. Abd El-Rahman RR, Harraz OF, Brett SE, et al. Identification of L- and T-type
417 Ca²⁺ channels in rat cerebral arteries: role in myogenic tone development. *Am J*
418 *Physiol Heart Circ Physiol.* 2013;304:H58–H71.
- 419 21. Perez-Reyes E. Molecular physiology of low-voltage-activated T-type calcium
420 channels. *Physiol Rev.* 2003;83:117–161.
- 421 22. Perez-Reyes E. Molecular characterization of T-type calcium channels. *Cell*
422 *Calcium.* 2006;40:89–96.
- 423 23. Hansen PB, Jensen BL, Andreassen D, Skøtt O. Differential expression of T- and
424 L-type voltage-dependent calcium channels in renal resistance vessels. *Circ Res.*
425 2001;89:630–638.
- 426 24. Jensen LJ, Salomonsson M, Jensen BL, Holte-Rathlou NH. Depolarization-
427 induced calcium influx in rat mesenteric small arterioles is mediated exclusively via
428 mibefradil-sensitive calcium channels. *Br J Pharmacol.* 2004;142:709–718.
- 429 25. Hayashi K, Wakino S, Homma K, Sugano N, Saruta T. Pathophysiological
430 significance of T-type Ca²⁺ channels: role of T-type Ca²⁺ channels in renal
431 microcirculation. *J Pharmacol Sci.* 2005;99:221–227.
- 432 26. Gustafsson F, Andreassen D, Salomonsson M, Jensen BL, Holstein-Rathlou N.
433 Conducted vasoconstriction in rat mesenteric arterioles: role for dihydropyridine-
434 insensitive Ca(2+) channels. *Am J Physiol Heart Circ Physiol.* 2001;280:H582–H590.
- 435 27. VanBavel E, Sorop O, Andreassen D, Pfaffendorf M, Jensen BL. Role of T-type
436 calcium channels in myogenic tone of skeletal muscle resistance arteries. *Am J*
437 *Physiol Heart Circ Physiol.* 2002;283:H2239–H2243.

- 438 28. Harraz OF, Abd El-Rahman RR, Bigdely-Shamloo K, et al. Ca(V)_{3.2} channels
439 and the induction of negative feedback in cerebral arteries. *Circ Res*. 2014;115:650–
440 661.
- 441 29. Morita H, Cousins H, Onoue H, Ito Y, Inoue R. Predominant distribution of
442 nifedipine-insensitive, high voltage-activated Ca²⁺ channels in the terminal
443 mesenteric artery of guinea pig. *Circ Res*. 1999;85:596–605.
- 444 30. Braunstein TH, Inoue R, Cribbs L, et al. The role of L- and T-type calcium
445 channels in local and remote calcium responses in rat mesenteric terminal arterioles.
446 *J Vasc Res*. 2009;46:138–151.
- 447 31. Peppiatt C, Lahne M, Howarth C, Attwell D, Mobbs P. Confocal imaging of
448 isolectin B4 labelling as a tool for studying neuronal-capillary interactions in living
449 cerebellar slices and retina from rats. *Proceedings of The Physiological Society: J*
450 *Physiol*. 2004;555P,PC21.
- 451 32. Scholfield CN, Curtis TM. Heterogeneity in cytosolic calcium regulation among
452 different microvascular smooth muscle cells in rat retina. *Microvasc Res*.
453 2000;59:233–242.
- 454 33. McGahon MK, Dawicki JM, Scholfield CN, McGeown JG, Curtis TM. A-type
455 potassium current in retinal arteriolar smooth muscle cells. *Invest Ophthalmol Vis*
456 *Sci*. 2005;46:3281–3287.
- 457 34. McDonald TF, Pelzer S, Trautwein W, Pelzer DJ. Regulation and modulation of
458 calcium channels in cardiac, skeletal, and smooth muscle cells. *Physiol Rev*.
459 1994;74:365–507.
- 460 35. Large WA, Wang Q. Characteristics and physiological role of Ca²⁺-activated Cl-
461 conductance in smooth muscle. *Am J Physiol*. 1996;271:C435–C454.
- 462 36. R Development Core Team. 2014. R: A language and environment for statistical
463 computing. R Foundation for Statistical Computing, Vienna, Austria. URL
464 <http://www.R-project.org/>
- 465 37. Nakanishi S, Kakita S, Takahashi I, et al. Wortmannin, a microbial product
466 inhibitor of myosin light chain kinase. *J Biol Chem*. 1992;267:2157–2163.
- 467 38. Burdyga TV, Wray S. The effect of inhibition of myosin light chain kinase by
468 Wortmannin on intracellular [Ca²⁺], electrical activity and force in phasic smooth
469 muscle. *Pflugers Arch*. 1998;436:801–803.
- 470 39. Fernández JA, Bankhead P, Zhou H, McGeown JG, Curtis TM. Automated
471 detection and measurement of isolated retinal arterioles by a combination of edge
472 enhancement and cost analysis. *PLoS One*. 2014;9:e91791.
- 473 40. Uebele VN, Gotter AL, Nuss CE, et al. Antagonism of T-type calcium channels
474 inhibits high-fat diet-induced weight gain in mice. *J Clin Invest*. 2009;119:1659–1667.
- 475 41. Kraus RL, Li Y, Gregan Y, et al. In vitro characterization of T-type calcium
476 channel antagonist TTA-A2 and in vivo effects on arousal in mice. *J Pharmacol Exp*
477 *Ther*. 2010;335:409–417.

- 478 42. Xiang Z, Thompson AD, Brogan JT, et al. The discovery and characterization of
479 ML218: a novel, centrally active T-type calcium channel inhibitor with robust effects
480 in STN neurons and in a rodent model of Parkinson's disease. *ACS Chem Neurosci*.
481 2011;2:730–742.
- 482 43. Navarro-Gonzalez MF, Grayson TH, Meaney KR, Cribbs LL, Hill CE. Non-L-Type
483 voltage-dependent calcium channels control vascular tone of the rat basilar artery.
484 *Clin Exp Pharmacol Physiol*. 2009;36:55–66.
- 485 44. Pluteanu F, Cribbs LL. Regulation and function of Cav3.1 T-type calcium
486 channels in IGF-I-stimulated pulmonary artery smooth muscle cells. *Am J Physiol*
487 *Cell Physiol*. 2011;300:C517–C525.
- 488 45. Chevalier M, Gilbert G, Roux E, et al. T-type calcium channels are involved in
489 hypoxic pulmonary hypertension. *Cardiovasc Res*. 2014;103:597–606.
- 490 46. Klöckner U, Lee JH, Cribbs LL, et al. Comparison of the Ca²⁺ currents induced
491 by expression of three cloned alpha1 subunits, alpha1G, alpha1H and alpha1I, of
492 low-voltage-activated T-type Ca²⁺ channels. *Eur J Neurosci*. 1999;11:4171–4178.
- 493 47. Kuo IY, Ellis A, Seymour VA, Sandow SL, Hill CE. Dihydropyridine-insensitive
494 calcium currents contribute to function of small cerebral arteries. *J Cereb Blood Flow*
495 *Metab*. 2010;30:1226–1239.
- 496 48. Kuo IY, Howitt L, Sandow SL, McFarlane A, Hansen PB, Hill CE. Role of T-type
497 channels in vasomotor function: team player or chameleon? *Pflugers Arch*.
498 2014;466:767–779.
- 499 49. Beltrame JF, Turner SP, Leslie SL, Solomon P, Freedman SB, Horowitz JD. The
500 angiographic and clinical benefits of mibefradil in the coronary slow flow
501 phenomenon. *J Am Coll Cardiol*. 2004;44:57–62.
- 502 50. Oshima T, Ozono R, Yano Y, et al. Beneficial effect of T-type calcium channel
503 blockers on endothelial function in patients with essential hypertension. *Hypertens*
504 *Res*. 2005;28:889–894.
- 505 51. Velat GJ, Kimball MM, Mocco JD, Hoh BL. Vasospasm after aneurysmal
506 subarachnoid hemorrhage: review of randomized controlled trials and meta-analyses
507 in the literature. *World Neurosurg*. 2011;76:446–454.
- 508 52. Björling K, Morita H, Olsen MF, et al. Myogenic tone is impaired at low arterial
509 pressure in mice deficient in the low-voltage-activated Ca_v 3.1 T-type Ca(2+)
510 channel. *Acta Physiol (Oxf)*. 2013;207:709–720.
- 511 53. Kuo IY, Wolfle SE, Hill CE. T-type calcium channels and vascular function: the
512 new kid on the block? *J Physiol*. 2011;589:783–795.
- 513 54. Hansen PB. Functional importance of T-type voltage-gated calcium channels in
514 the cardiovascular and renal system: news from the world of knockout mice. *Am J*
515 *Physiol Regul Integr Comp Physiol*. 2015;308:R227–R237.
- 516 55. Takahashi T, Nagaoka T, Yanagida H, et al. A mathematical model for the
517 distribution of hemodynamic parameters in the human retinal microvascular network.
518 *J Biorheol*. 2009;23:77–86.

519 56. Arciero J, Harris A, Siesky B, et al. Theoretical Analysis of Vascular Regulatory
520 Mechanisms Contributing to Retinal Blood Flow Autoregulation. *Invest Ophthalmol*
521 *Vis Sci.* 2013;54:5584–5593.

522 57. Jeppesen P, Aalkjaer C, Bek T. Myogenic response in isolated porcine retinal
523 arterioles. *Curr Eye Res.* 2003;27:217–222.

524 58. Harraz OF, Brett SE, Welsh DG. Nitric oxide suppresses vascular voltage-gated
525 T-type Ca²⁺ channels through cGMP/PKG signaling. *Am J Physiol Heart Circ*
526 *Physiol.* 2014;306:H279–H285.

527 59. Cazade M, Bidaud I, Hansen PB, Lory P, Chemin J. 5,6-EET potently inhibits T-
528 type calcium channels: implication in the regulation of the vascular tone. *Pflugers*
529 *Arch.* 2014;466:1759–68.

530 60. Park JY, Kang HW, Moon HJ, et al. Activation of protein kinase C augments T-
531 type Ca²⁺ channel activity without changing channel surface density. *J Physiol.*
532 2006;577:513–23.

533 61. Tzeng BH, Chen YH, Huang CH, Lin SS, Lee KR, Chen CC. The Ca(v)3.1 T-type
534 calcium channel is required for neointimal formation in response to vascular injury in
535 mice. *Cardiovasc Res.* 2012;96:533-542.

536
537
538
539
540
541
542
543
544
545
546
547
548
549
550
551
552

553 **Figure legends**

554 **Figure 1.** (A) Arteriole and (B) venule within a retinal wholemount preparation
555 immunolabelled for α -SMA (red channel). Nuclei were labelled with the far-red
556 nuclear stain TOPRO3 (pseudo-coloured blue).

557 **Figure 2.** Distribution patterns of $Ca_v3.1-3$ T-type channel isoforms in retinal
558 arterioles and the surrounding retinal parenchyma (A) Top panel, rat retinal
559 wholemount preparation immunolabelled for $Ca_v3.1$ (green channel), α SMA (red
560 channel) and cell nuclei (blue channel; TOPRO3). Bottom panel, $Ca_v3.1$ staining
561 segmented from the same image. (B) Individual and merged images showing $Ca_v3.1$
562 (green channel) co-localisation with the plasma membrane marker, isolectin B4 (red
563 channel), in retinal arteriolar myocytes. (C) Top panel, secondary only control image.
564 Bottom panel, blocking peptide experiment for the anti- $Ca_v3.1$ primary antibody. (D,
565 E) Equivalent immunolabelling to that shown in A, but for $Ca_v3.2$ and $Ca_v3.3$
566 isoforms, respectively.

567 **Figure 3.** (A) TTA-A2-sensitive T-type currents (left panel) and nimodipine-sensitive
568 L-type currents (right panel) elicited in response to voltage steps from -80 to +40mV
569 in 10 mV increments from a holding potential of -80 mV. Current traces are
570 presented as difference currents. (B) Representative (left) and mean (right) *I-V*
571 relationships (n=8 cells) for the TTA-A2 and nimodipine-sensitive currents. (C)
572 Kinetic rate constants of activation and inactivation for the currents obtained in A.
573 Analysis was carried out on currents obtained at a voltage step to -10 mV (left
574 panel). Dashed boxes indicate both the activation (magnified in the middle panel)
575 and inactivation (magnified in the right panel) of the currents at that voltage.

576 Activating and inactivating currents were fitted using single exponentials. (D) Mean
 577 time constants of activation (left) and inactivation (right) (n=8).

578 **Figure 4.** Effects of T-type blockers on the diameter of isolated retinal arterioles
 579 under myogenic tone. (A) Representative traces showing the diameters of vessels
 580 under steady-state myogenic tone (grey line, actual diameter; black line, smoothed
 581 trace showing the moving average of 11 points superimposed on top of the raw
 582 diameters) at an intraluminal pressure of 40 mmHg (first 2–3 minutes), dilation of the
 583 vessel after application of the T-type blocker (TTA-A2, 1 μ M, left panel; ML-218, 1
 584 μ M, right panel), and subsequent further dilation to the maximal passive diameter
 585 after application of wortmannin in Ca^{2+} -free Hanks' solution. (B) Mean arteriole
 586 diameters normalised to the maximal diameters following application of DMSO, TTA-
 587 A2 or ML-218.

588

589 **Table 1.** Antibodies and dilutions used to investigate $Ca_v3.1-3$ protein expression.

Protein	Antibody (Company)	Epitope(species)	Dilution
$Ca_v3.1$	ACC-021 (Alomone; Jerusalem, Israel)	AA1–22 (rat)	1:200
$Ca_v3.2$	ACC-025 (Alomone)	AA581–595 (human)	1:200
$Ca_v3.3$	OSC00263W (Osenses; Keswick, Australia)	AA450-500 (human)	1:200

590

591 **Table 2.** Effects of T-type blockers on the diameters of pressurised retinal arterioles.

Diameters (μ m)	After steady-state tone development	In presence of vehicle/inhibitor	Passive diameter	% diameter change
DMSO (n=10)	29.5 \pm 1.6	29.4 \pm 1.5	30.6 \pm 1.4	N/A
TTA-A2 (n=16)	29.1 \pm 2.4	29.6 \pm 2.5	30.1 \pm 2.5	45.4 \pm 3.9
ML-218 (n=13)	31.3 \pm 2.7	31.8 \pm 2.7	32.3 \pm 2.7	54.1 \pm 4.2

592

Figure 1

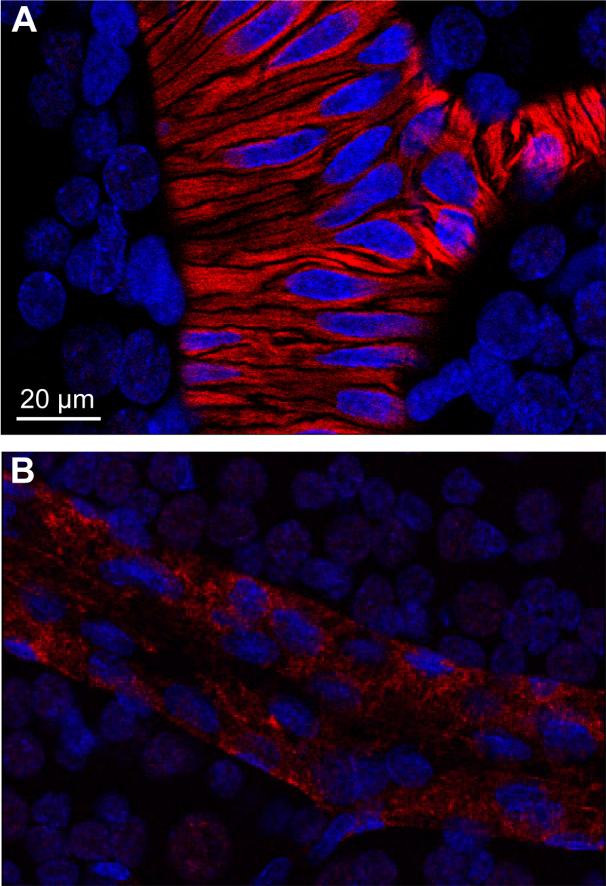


Figure 2

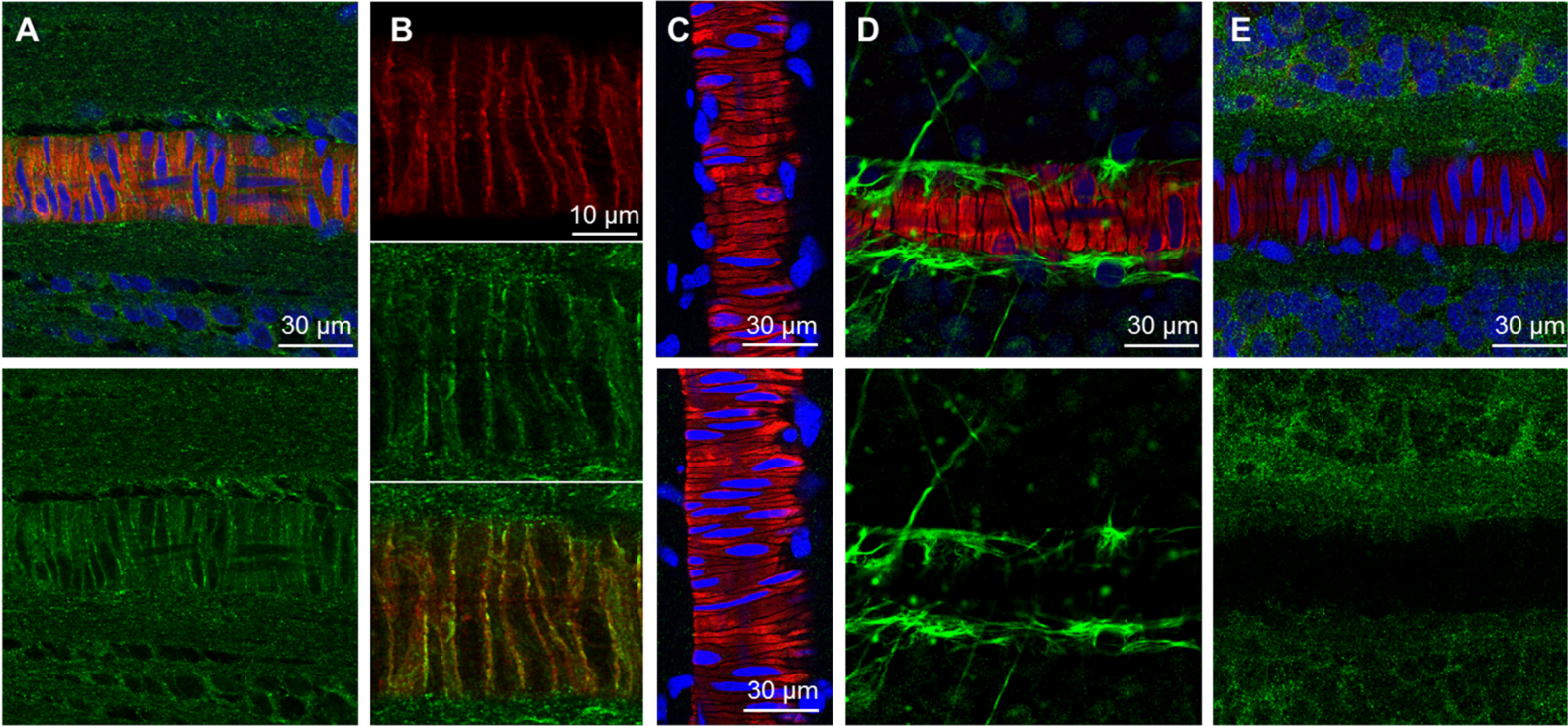


Figure 3

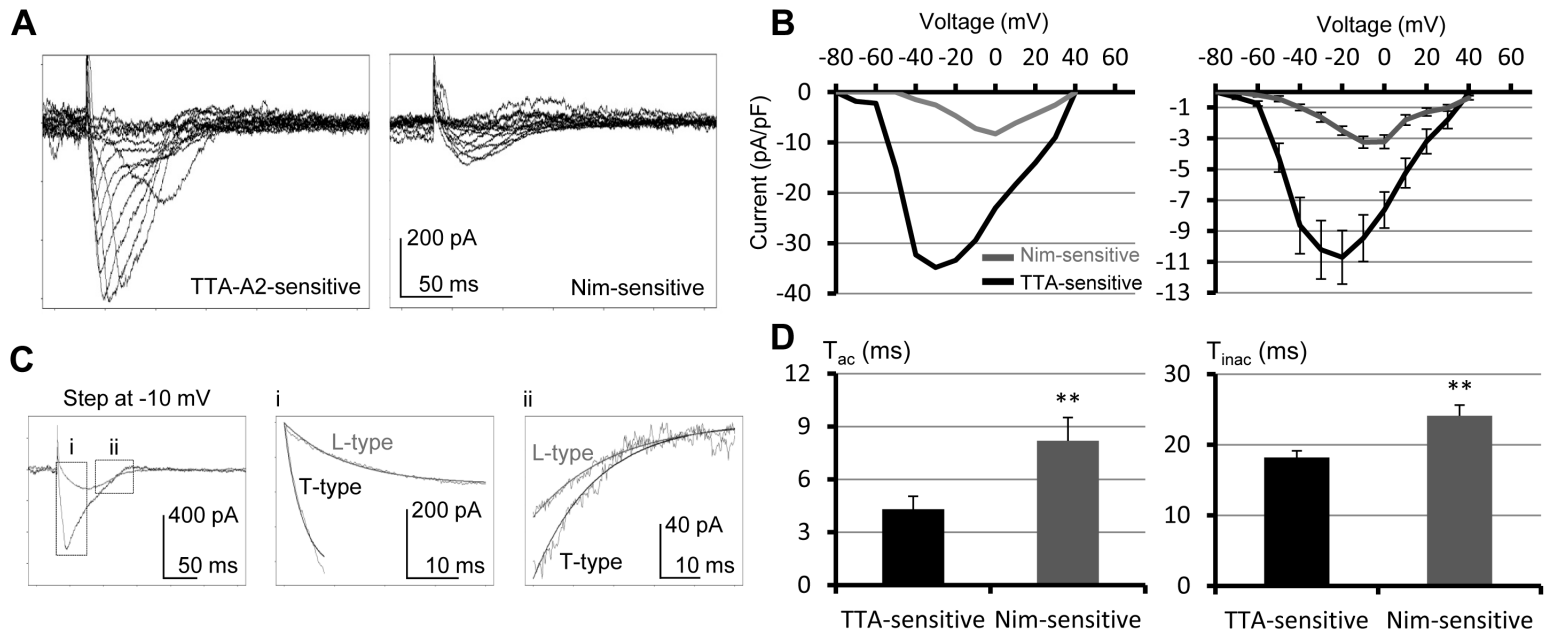


Figure 4

